

**Localization of the 5-HT<sub>1A</sub> receptor in lipid microdomains depends on its  
palmitoylation and is involved in receptor-mediated signalling**

Ute Renner, Konstantin Glebov, Thorsten Lang, Ekaterina Papusheva, Saju Balakrishnan,  
Bernhard Keller, Diethelm W. Richter, Reinhard Jahn, Evgeni Ponimaskin

U.R., K.G., E.P., S.B., B.K., D.W.R. and E.P., Abteilung Neuro- und Sinnesphysiologie,  
Physiologisches Institut, Universität Göttingen, Humboldtallee 23, 37073 Göttingen,  
Germany; U.R., D.W.R. and E.P., Center of Molecular Physiology of the Brain, Göttingen,  
Germany; T.L. and R.J., Department of Neurobiology, Max-Planck-Institute for Biophysical  
Chemistry, D37077 Göttingen, Germany.

**Running Title:**

**Palmitoylation and raft localization of the 5-HT<sub>1A</sub> receptor**

**To whom correspondence should be addressed:**

Evgeni Ponimaskin. Abteilung Neuro- und Sinnesphysiologie, Physiologisches Institut, Universität Göttingen, Humboldtallee 23, D-37073 Göttingen, Germany; Tel. 49-551-395939, Fax: 49-551-396031; E-mail: eponima@gwdg.de

The number of text pages: **36**

The number of tables: **0**

The number of figures: **9**

The number of references: **62**

The number of words in the *Abstract*: **188**

The number of words in the *Introduction*: **724**

The number of words in the *Discussion*: **1.347**

**List of Abbreviations**

5-HT<sub>1A</sub>, mouse 5-hydroxytryptamine(1A) receptor; CTX, cholera toxin; CFP, cyan fluorescent protein; DRM, detergent-resistant membrane fraction; DMEM, Dulbecco's modified Eagle's medium; GPCR, heterotrimeric GTP-binding protein-coupled receptor; M $\beta$ CD, methyl- $\beta$ -cyclodextrin; PTx, pertussis toxin; YFP, yellow fluorescent protein.

MOL #037085

## ABSTRACT

In the present study we have utilized wild-type and palmitoylation-deficient 5-HT1A receptors fused to the yellow fluorescent protein (YFP) as well as cyan fluorescent protein (CFP)-tagged  $\alpha_{i3}$ -subunit of heterotrimeric G-protein to study spatio-temporal distribution of the 5-HT1A-mediated signaling in living cells. We also addressed the question on the molecular mechanisms by which receptor palmitoylation may regulate communication between receptors and  $G_i$ -proteins. Our data demonstrate that activation of the 5-HT1A receptor caused a partial release of  $G_{\alpha_i}$  protein into the cytoplasm and that this translocation is accompanied by significant increase of the intracellular  $Ca^{2+}$  concentration. In contrast, acylation-deficient 5-HT1A mutants failed to reproduce both  $G_{\alpha_{i3}}$ -CFP relocation as well as changes in  $[Ca^{2+}]_i$  upon agonist stimulation. By using gradient centrifugation and co-patching assays, we also demonstrate that a significant fraction of the 5-HT1A receptor resides in membrane rafts, while the yield of the palmitoylation-deficient receptor in these membrane microdomains is considerably reduced. Our results suggest that receptor palmitoylation serves as a targeting signal responsible for the retention of the 5-HT1A receptor in membrane rafts. More importantly, the raft localization of the 5-HT1A receptor appears to be involved in receptor-mediated signaling.

## INTRODUCTION

G-protein-coupled receptors (GPCRs) play a central role in transducing extracellular signals across the cell membrane with high sensitivity and specificity. These integral membrane proteins represent the largest and most versatile group of receptors with an essential role in the regulation of almost all physiological processes in both mammalian and non-mammalian species (Pierce et al., 2002). A large body of evidence obtained in different experimental systems suggests that the specificity of GPCR-mediated signalling is partially achieved by the selective compartmentalization of signalling components within specific microdomains on the plasma membrane (Anderson, 1998; Chini and Parenti, 2004). These microdomains, named lipid rafts and caveolae, represent the membrane subdomains differing from the bulk membrane by enrichment in specific proteins and lipids. They are characterised by a high content of glycosphingolipid and cholesterol in the outer leaflet of the lipid bilayer that gives them a gel-like liquid-ordered ( $l_o$ ) structure (Brown and London, 1998). In contrast to the membranes in the conventional disordered phase, lipid rafts and caveolae are resistant to the low-temperature solubilization by non-ionic detergents (Brown and London, 1998) allowing for their biochemical separation due to the differential flotation in the density gradients.

Lipid rafts and caveolae have been shown to be involved in the regulation of various cell functions including the intracellular sorting of proteins and lipids (Sprong et al., 2001), the establishment of cell polarity (Manes et al., 2003) and the fine tuning of signalling processes (Simons and Toomre, 2000). The detection of numerous signalling proteins within the detergent-resistant membrane fractions (DRMs) led to the assumption that lipid rafts represent scaffold platforms which facilitate signal transduction by spatially recruiting signalling components and by preventing an inappropriate cross-talk between pathways (Foster et al., 2003; Okamoto et al., 1998). Little is known about the molecular determinants regulating localization of signalling proteins and particularly GPCRs in lipid microdomains. Several possible mechanisms for rafts targeting have been proposed including (*i*) specific interaction

MOL #037085

with the lipid components of rafts/caveolae such as cholesterol (Eroglu et al., 2003) (Pucadyil and Chattopadhyay, 2004), (ii) direct interaction with the scaffolding domain of caveolin (Okamoto et al., 1998) and (iii) the covalent attachment of saturated fatty acyl chains, including myristic and palmitic acids (Moffett et al., 2000; Zacharias et al., 2002).

In the present study we have utilized wild-type and palmitoylation-deficient 5-HT<sub>1A</sub> receptors tagged to the yellow fluorescent protein (YFP) as well as cyan fluorescent protein (CFP)-tagged  $\alpha_i$ -subunit of heterotrimeric G-protein (Leaney et al., 2002) to study spatio-temporal distribution of the 5-HT<sub>1A</sub>-mediated signalling. In addition we analysed, whether receptor palmitoylation is involved in targeting the receptor to the membrane subdomains.

The 5-HT<sub>1A</sub> receptor belongs to the GPCR superfamily and is the most extensively characterised member of the serotonin (5-hydroxytryptamine or 5-HT) receptor family. This receptor was found to be involved in a number of physiological and behavioral effects, such as regulation of mood (Sibille and Hen, 2001), neuroendocrine responses (Burnet et al., 1996), body temperature (Overstreet, 2002), neurogenesis (Radley and Jacobs, 2002) and respiratory activity (Richter et al., 2003). The 5-HT<sub>1A</sub> receptor has also been shown to play an important role in several psychiatric disorders, and its partial agonists are widely used in the treatment of depression and anxiety syndromes (Gordon and Hen, 2004).

The 5-HT<sub>1A</sub> receptor is coupled to a variety of effectors via pertussis toxin sensitive G-proteins of the G<sub>i/o</sub> family (De Vivo and Maayani, 1986; Dumuis et al., 1988). Receptor-induced activation of G $\alpha_i$ -subunits results in the inhibition of adenylyl cyclase and a subsequent decrease of cAMP levels in both homologous and heterologous systems (De Vivo and Maayani, 1986; Nebigil et al., 1995). Besides effects mediated by G $\alpha_{i/o}$  subunits, activation of the 5-HT<sub>1A</sub> receptor also leads to the G $\beta\gamma$ -mediated activation of K<sup>+</sup> currents, stimulation of phospholipase C as well as activation of mitogen-activated protein kinase Erk2 (Andrade et al., 1986; Fargin et al., 1991; Garnovskaya et al., 1996).

MOL #037085

We have recently shown that the recombinant 5-HT<sub>1A</sub> receptor is modified by covalently attached palmitate and that palmitoylation of the 5-HT<sub>1A</sub> receptor is irreversible and insensitive to agonist stimulation (Papoucheva et al., 2004). Two conserved cysteine residues 417 and 420 located in the C-terminal domain were identified as acylation sites of the 5-HT<sub>1A</sub> receptor. When palmitoylated cysteines were mutated, communication between receptors and G $\alpha_i$ -subunits was completely abolished, indicating that palmitoylation of the 5-HT<sub>1A</sub> receptor is critical for G<sub>i</sub>-protein coupling/effector signalling (Papoucheva et al., 2004).

## MATERIALS AND METHODS

### *Recombinant DNA procedures*

All basic DNA procedures were performed as described by Sambrook et al. (Sambrook, 1989). The  $G\alpha_{i3}$ -CFP cDNA was kindly provided by Dr. Andrew Tinker (London, UK). The construction of the HA-tagged 5-HT1A as well as generation of the palmitoylation-deficient 5-HT1A mutant (C417-S, C420-S) has been described previously (Papoucheva et al., 2004). To prepare a 5-HT1A-YFP fusion construct, cDNA encoding for the 5-HT1A receptor was amplified by PCR with the specific primer *Chimera sense-KpnI* (5'-ATTCCGGTACCGCGAGGGAGATCCCCTTG-3') and either with *Chimera antisense WT-KpnI* (5'-ATCATGGTACCGGGCGGCAGAACTTGCAC-3') for wild-type or *Chimera antisense DM-KpnI* (5'-ATCATGGTACCGGGCGGGAGA AACTTGGAC-3') for acylation-deficient mutant. The amplified fragments were cloned into the KpnI site of the pEYFP-N1 vector (Clontech), so that the YFP coding sequence was located in-frame at the C-terminal end of the 5-HT1A receptor. All constructs were verified by dideoxy DNA sequencing of the final plasmids.

### *Adherent cell culture and transfection*

NIH-3T3 and neuroblastoma N1E-115 cells were grown in Dulbecco's modified Eagle's medium (DMEM) containing 10% fetal calf serum (FCS) and 1% penicillin/streptomycin at 37°C under 5% CO<sub>2</sub>. For transient transfection, cells were seeded at low-density ( $8 \times 10^5$ ) in 35-mm dishes or in 10-mm cover-slips ( $5 \times 10^5$ ) and transfected with appropriate vectors using Lipofectamine2000 Reagent (Invitrogen) according to the manufacturer's instruction. Six hours after transfection cells were serum starved for different time intervals before analysis. To prepare the cell line stably expressing YFP-tagged receptor, the NIH-3T3 cells were seeded into 35-mm dishes and transfected either with the wild-type or acylation-deficient 5-HT1A-YFP constructs. After two weeks incubation in the selective medium containing

Geneticin (1 mg/ml; Invitrogen), single colonies were collected and plated on separate 60 mm dishes. The stably transfected cell lines were tested for the expression level of the recombinant protein by immunoblotting and radioligand binding assay.

### ***Biotinylation and isolation of cell surface proteins***

For biotinylation assay, transiently transfected N1E-115 cells ( $5 \times 10^6$ ) expressing HA- or YFP-tagged 5-HT<sub>1A</sub> receptors were treated according to the manufacturer's protocol (PIERCE). Briefly, cells were washed three times with ice-cold PBS and incubated for 30 min at 4°C in PBS (100 mM NaPO<sub>4</sub>, 150 mM NaCl; pH 7.2) containing 0.25 mg/ml sulfo-NHS-SS-Biotin. Cells were harvested, centrifuged at 500 x g for 5 min and washed with ice-cold TBS (25 mM Tris, 150 mM NaCl; pH 7.2). The cells were lysed, and lysates were cleared by centrifugation at 10,000 x g for 2 min. The biotinylated proteins were isolated from the supernatant with immobilized NeutrAvidin™ during 1 h incubation at room temperature. Biotinylated proteins were eluted with 50 µl of SDS sample buffer containing 50 mM DTT. Biotinylated as well as unbound proteins were separated by 12% SDS-PAGE followed by immunoblotting with anti-HA (SantaCruz) or anti-GFP (Abcam) antibodies.

### ***Assay for [Eu]-GTPγS binding***

Agonist-promoted binding of [Eu]-GTPγS (Eu, Europium) to Gα<sub>i</sub> protein was performed according to the method described by Barr et al. (Barr et al. 1997). Briefly, 10 µg of membranes from transfected N1E-115 cells were resuspended in 55 µl of 50 mM Tris-HCl buffer (2 mM EDTA, 100 mM NaCl, 3 mM MgCl<sub>2</sub>, 1 µM GDP; pH 7.4) and incubated without or with different concentrations of 8-OH-DPAT at room temperature for 10 min. In several experiments, WAY100635 at 1 µM concentration was added to the membranes 5 min before agonist. After adding [Eu]-GTPγS (PerkinElmer) to a final concentration of 10 nM, samples were incubated for 1.5 h at room temperature. The reaction was terminated by adding

MOL #037085

600  $\mu$ l of 50 mM Tris-HCl (pH 7.5) containing 20 mM MgCl<sub>2</sub>, 150 mM NaCl, 0.5% NP-40, 200  $\mu$ g/ml aprotinin, 100  $\mu$ M GDP and 100  $\mu$ M GTP and incubated for 15 min on the ice. The samples were then incubated for 1.5 h with 10  $\mu$ l of antibody raised against G $\alpha_{i3}$  protein (SantaCruz) followed by 1.5 h incubation with 30  $\mu$ l of Sepharose-ProteinG beads (Sigma). Immunoprecipitates were washed, heated at 37°C for 15 min in 0.2 ml of 0.5% SDS, centrifuged, and supernatants were subjected to the fluorescence detection. Fluorescence of Eu was measured using fluorescent plate reader MithrasLB680 (Berthold) at excitation of 315 nm and emission of 615 nm. The data were fitted to a sigmoidal function and analyzed using Matlab software (The MathWork, Stuttgart, Germany).

### **Erk1/2 phosphorylation assay**

Serum starved, transiently or stably transfected NIH-3T3 cells ( $7 \times 10^5$ ) were stimulated for 5 minutes with 10  $\mu$ M 8-OH-DPAT, washed with PBS and lysed in loading buffer. Equal amounts of proteins in lysates were separated by SDS/PAGE and then subjected to immunoblot. The membranes were probed either with antibodies raised against phosphorylated Erk1/2 (phospho-p42/44; 1:2000 dilution) or against total Erk (p42/44; 1:1000 dilution). To compare the level of receptor expression, membranes were probed with antibodies raised against GFP (1:500; Abcam). Amount of the phosphorylated and the total Erk1/2 were quantified by densitometric measurements using GelPro Analyser version 3.1 software.

### ***Radioligand binding assay***

Membrane preparation of transiently or stably transfected cells was performed according to the protocol described by Claeysen and co-workers (Claeysen et al., 1999). For saturation binding assay indicated concentrations of 8-OH-[<sup>3</sup>H]-DPAT (Amersham) were added to 10  $\mu$ g of the membrane fraction diluted in assay buffer (20 mM HEPES pH 7.4, 1 mM EDTA, 1

MOL #037085

mM EGTA, 6 mM MgCl<sub>2</sub> and 0,1% BSA). The final volume was 200 µl and non-specific binding was determined by addition of 10 µM unlabelled 5-HT. After 2.5-h incubation at 20° C, the reaction was terminated by rapid filtration of the samples through GF/B filters (Whatman) presoaked in 1% polyethylenimine using a Brandel cell harvester. The membranes were washed 4 times with ice-cold PBS and the radioactivity was measured by scintillation counter. Data were fitted with the one-site saturation binding model by pharmacology module of SigmaPlot 8.02 software.

***Ca<sup>2+</sup> imaging***

For intracellular calcium measurements, 5 µM Fura-2AM (Molecular Probes) was added to serum free culture medium containing 100 ng/ml pertussis-toxin and cells were incubated for 60 min at 37°C under 5% CO<sub>2</sub>. Fluorescence measurements of the cells were done in artificial cerebrospinal fluid (118 mM NaCl, 3 mM KCl, 1 mM MgCl<sub>2</sub>, 25 mM NaHCO<sub>3</sub>, 1mM NaH<sub>2</sub>PO<sub>4</sub>, 1.5 mM CaCl<sub>2</sub> and 30 mM Glucose, pH 7.4), bubbled with carbogen. Receptors were stimulated by adding 8-OH-DPAT (30 µM) to the bath solution. Fura-2AM was alternately excited and 356 nm and 385 nm, emitted light was directed to a dichroic mirror with mid-reflection at 425 nm, filtered by a band pass filter (505-530 nm) and collected using a CCD camera (Sensicam). Fluorescence values were calculated as ratio of fluorescence intensities F/F<sub>0</sub>.

***Cell fractionation and immunoblotting***

Transiently transfected neuroblastoma N1E-115 cells expressing 5-HT1A-YFP and Gα<sub>i3</sub>-CFP constructs were incubated with 100 ng/ml pertussis-toxin (Sigma) during the serum starvation. After stimulation with 30 µM 8-OH-DPAT for 30 s, cells were immediately harvested in ice-cold extraction buffer (10 mM Tris/HCl pH 7.4, 1 mM EDTA, 150 mM NaCl, 1 mM DTT, 20 µM Leupeptin, 2µg Aprotinin/ml) and homogenized. After

MOL #037085

centrifugation at 8,500 rpm for 5 min, supernatant was centrifuged at 60,000 rpm at 4°C for 30 min on the Beckman-Coulter ultracentrifuge with TLA120.2 rotor to separate membrane and cytosolic fraction. The pellets and the supernatants (the latter after extraction with 10% TCA) were separated by 10% SDS-PAGE. Proteins were transferred to Hybond nitrocellulose membrane (Amersham) and probed either with antibodies raised against  $G\alpha_{i3}$  (Santa Cruz; 1:1000 diluted in PBS/Tween20) or against GFP (Abcam; diluted 1:5000 in PBS/Tween20). Proteins were detected using the enhanced chemiluminescence detection reagents (Amersham Biosciences).

***Time-lapse confocal microscopy***

Neuroblastoma N1E-115 cells were co-transfected with  $G\alpha_{i3}$ -CFP and 5-HT1A-YFP constructs at the DNA ratio 2:1 or 4:1, incubated with 100 ng/ml pertussis toxin (Sigma) during the serum starvation and then monitored under an inverted confocal laser-scan microscope LSM510-Meta (Zeiss, Jena, Germany) with a 63x 1,2NA water-immersion objective using 458 nm line of an argon laser. Experiments were performed at 37°C in Tyrode's buffer (150 mM NaCl, 10 mM HEPES, 10 mM Glucose, 5 mM KCl, 2 mM  $CaCl_2$ , 1 mM  $MgCl_2$ , 100 ng/ml PTx, pH 7.4). For receptor stimulation, 8-OH-DPAT at final concentration of 30  $\mu$ M was added to the bath. For detection of individual fluorophores, spectral range for lambda stack acquisition was set from 462 nm to 580 nm, yielding a 12 image stacks with 10.7 nm increments. The reference spectra of CFP- and YFP-chimera were recorded for each experiment from the cells expressing the individual construct, and the spectral separation was achieved by the linear unmixing function of the LSM Meta software. In the time-laps analysis, 1  $\mu$ m optical z-sections were captured at each time point before and during treatment with 8-OH-DPAT. The time interval between successive scans was 10 s. For quantitative analysis of  $G\alpha_i$ -CFP distribution, z-sections were projected onto one plane and the region of interest corresponding to the maximal cytoplasm area was selected for each cell.

MOL #037085

Changes in CFP-fluorescence intensity were determined from the equation:  $(F_{\text{post}} - F_{\text{pre}}) \times 200 / F_{\text{pre}}$ , where  $F_{\text{pre}}$  and  $F_{\text{post}}$  are the mean of fluorescence intensity before and during agonist treatment, respectively. Multiplication by 200 was used to span the greyscale spectrum of 8-bit images. Prior to calculations, images were smoothed using a low pass Gaussian filter of a 7x7 pixel kernel. Statistical evaluation was performed using the paired t-test applied to compare the averaged values derived from at least three independent experiments.

***Gradient centrifugation***

Separation of detergent-resistant membranes derived from the stably transfected NIH-3T3 cells ( $1 \times 10^6$ ) and transiently transfected CHO cells ( $1 \times 10^6$ ) growing on 35 mm dishes was performed as described by Harder and co-workers (Harder et al., 1998). For cholesterol depletion, cells were washed twice with culture medium without FCS and antibiotics and treated with 15 mM methyl- $\beta$ -cyclodextrin for 45 min on ice. Cells were lysed in TNE buffer (25 mM Tris/HCl, pH7.4, 150 mM NaCl, 5 mM EDTA, 1 mM DTT, 10% sucrose, 1% Triton X-100, 1 mM PMSF, 10  $\mu$ M Leupeptin, 2  $\mu$ g/ml Aprotinin) and lysates (1.2 mg protein/ml) were mixed with the double volume of 60% Optiprep<sup>TM</sup> gradient medium (Nycomed Pharma). The resulting 40% Optiprep<sup>TM</sup> mixture was transferred into the ultracentrifuge tube and overlaid with steps of each 35%, 30%, 25%, 20% and 0% Optiprep<sup>TM</sup> in TNE. The gradients were centrifuged for 5 h at 50.000 rpm in the TLS-55 rotor of the ultracentrifuge TL-100 (Beckman). Six fractions were collected from the top of the gradient and TCA-precipitated. The pellets were analysed by SDS-PAGE followed by immunoblot analysis with appropriate antibodies.

***Copatching assay and line scan analysis***

MOL #037085

For preparation of membrane sheets, stably transfected NIH-3T3 cells were treated according to Avery and co-workers (Avery et al., 2000). Copatching of YFP-fused receptors and GM1 was carried out by simultaneous incubation of unfixed membrane sheets with goat anti-GFP antibody (Abcam; 1:1000 dilution) and cholera-toxin (Sigma, 1 $\mu$ g/ml). Incubation was performed in KGlu buffer (120 mM K-glutamate, 20 mM K-acetate, 20 mM HEPES pH7.2) containing 0.5% BSA for 60 min at 37°C. Membranes were washed and fixed in 4% PFA for 60 min. The fixed sheets were incubated with mouse anti-CTX antibodies with 1:1000 dilution, followed by incubation with Alexa Fluor 546-conjugated rabbit anti-mouse antibody (1:500). Before imaging, membranes were stained with TMA-DPH which was directly added to the bath solution. For cholesterol depletion, membrane sheets were treated for 10 min with 5 mM methyl- $\beta$ -cyclodextrin (Sigma) in KGlu buffer prior copatching. For the line scan analysis membrane sheets were imaged using Zeiss Axiovert 100 TV fluorescence microscope with a 100x 1.4 NA Plan-Achromate objective and a back-illuminated frame transfer CCD-camera. Membrane sheets were imaged in three channels, blue for TMA-DPH (430 nm), green for 5-HT1A-YFP (515 nm) and red for Alexa546-CTX (546 nm). Red and green channels were aligned by color align function of MetaMorph software (Universal Imaging, West Chester, PA, USA) using fluorescent beads (TetraSpec microspheres 0.2  $\mu$ m, Molecular Probes) which have been added to every membrane preparation.

For co-localization analysis, 20 lines (25 pixels/line) per image were drawn across clustered receptors, while red channel was switched off. Distance between maximal intensities of red and green pixels in each line was determined on the merge pictures using line scan function of the MetaMorph software and when the distance was less than two pixels, a co-localization event was counted. For normalization, the counting protocol was repeated after horizontal flipping of the red channel.

## RESULTS

### *Generation and functional properties of 5-HT1A-YFP fusion constructs*

To study 5-HT1A receptor-mediated signalling processes in living cells, enhanced yellow fluorescence protein (YFP) was fused to the C-terminal domain of the wild-type (WT-YFP) and acylation-deficient (Mut-YFP) 5-HT1A receptors after removing the stop codon (Fig. 1A). Immunoblot analysis performed in transfected neuroblastoma N1E-115 cells revealed a protein band with a predicted molecular weight of approximately 76 kDa for both WT-YFP and Mut-YFP constructs (Fig. 1B).

To exclude the possibility that fusion to the YFP alters receptor properties, we analysed the subcellular distribution, pharmacological profile as well as downstream signalling of the fluorescent-labelled receptors by comparison with the HA-tagged 5-HT1A receptors (Papoucheva et al., 2004). Cellular location of YFP-tagged receptors was firstly analysed by the biotinylation assay. For that intact cells expressing 5-HT1A receptors were labelled with a membrane impermeable sulfo-NHS-biotin, and biotinylated proteins from plasma membranes were purified by streptavidin. Finally, receptors were revealed by immunoblotting using anti-HA or anti-GFP antibodies. As shown in figure 1C, both HA- and YFP-tagged 5-HT1A receptors were purified by streptavidin-agarose, suggesting that these receptors are expressed at the cell surface.

Confocal microscopy performed after transfection of WT-YFP or Mut-YFP constructs into N1E-115 cells also demonstrated that the major part of the YFP-tagged receptors was on the plasma membranes with only a minor fraction presented in the intracellular compartments (Fig. 1D). The predominant localization of WT-YFP and Mut-YFP fusion proteins at the plasma membrane was also confirmed in transiently as well as stably transfected NIH-3T3 cells (data not shown).

The pharmacological profiles of the WT-YFP and Mut-YFP constructs were analysed by saturation binding of the selective 5-HT1A receptor agonist [<sup>3</sup>H]8-OH-DPAT in the

MOL #037085

membrane preparations from transfected NIH-3T3 cells (Fig. 2A). The binding affinities of [<sup>3</sup>H]8-OH-DPAT for WT-YFP ( $K_D = 0.72 \pm 0.53$  nM) and Mut-YFP ( $K_D = 0.97 \pm 0.26$  nM) were similar to that obtained for the HA-tagged receptors ( $K_D = 0.76 \pm 0.23$  nM). These values are also in accordance with those previously reported for recombinant and native 5-HT<sub>1A</sub> receptors (Newman-Tancredi et al., 1998; Pucadyil et al., 2004), demonstrating that the YFP fusion does not change the receptor's pharmacological properties.

The ability of YFP-tagged receptors to stimulate G-protein activity was then analyzed by the fluorescence-based GTP $\gamma$ S assay performed on the membrane preparations from transfected N1E-115 cells in the presence or in the absence of 8-OH-DPAT. The binding specificity to the inhibitory G-proteins was provided by the immunoprecipitation of membrane preparations with anti-G $\alpha_{i3}$  antibody before the fluorescence measurement. As shown in figure 2B, activation of the HA-tagged receptor with 100  $\mu$ M 8-OH-DPAT elicited an approximately 3.7-fold increase in [Eu]GTP $\gamma$ S binding. Activation of YFP-tagged 5-HT<sub>1A</sub> receptors resulted in the similar stimulation of GTP $\gamma$ S binding (Fig. 2B). In contrast, no stimulation of [Eu]GTP $\gamma$ S binding was observed in membranes of non-transfected cells (data not shown). When the ability of non-palmitoylated YFP-tagged 5-HT<sub>1A</sub> receptor mutant to stimulate [Eu]GTP $\gamma$ S binding was analyzed, we found that the relative activation of G $\alpha_{i3}$ -subunit after agonist stimulation in this case was completely abolished (Fig. 2B). This was in line with our previous data obtained for acylation-deficient HA-tagged receptor (Papoucheva et al., 2004). It is also notable that treatment of HA- and YFP-tagged receptors with 8-OH-DPAT resulted in a dose-dependent increase of GTP $\gamma$ S binding to G $\alpha_{i3}$  proteins with very similar EC<sub>50</sub> values (HA-WT,  $1 \pm 0.8$   $\mu$ M; WT-YFP,  $3 \pm 2$   $\mu$ M) (Fig. 2C). Parallel treatment of the membrane preparation from cells expressing YFP- or HA-tagged 5-HT<sub>1A</sub> receptors with the selective receptor antagonist WAY100635 at 1 $\mu$ M concentration completely

antagonized [Eu]GTP $\gamma$ S binding, indicating specific involvement of 5-HT1A in G $\alpha_{i3}$  activation (Fig. 2C).

In addition to G $\alpha_i$ -mediated inhibition of the adenylyl cyclases, the 5-HT1A receptor has been shown to modulate the activity of the extracellular signal-regulated kinase (Erk) via a G $\beta\gamma$ -mediated pathway (Cowen et al., 1996; Garnovskaya et al., 1996). Previously, we have demonstrated that agonist stimulation of the wild-type 5-HT1A receptor resulted in activation of Erk, while receptor-mediated activation of Erk was significantly impaired after expression of non-acylated mutant (Papoucheva et al., 2004). To prove the functionality of WT-YFP and Mut-YFP receptors, we analysed their ability to modulate the Erk activation. As shown in Figure 3A and 3B, agonist treatment of N1E-115 cells transfected with HA- or YFP- tagged wild-type receptors resulted in an approximately 8 or 9 fold increase in Erk phosphorylation, respectively. In the case of HA-tagged acylation-deficient mutant and Mut-YFP, receptor stimulation induced only a weak increase in phosphorylation of Erk (approx. 2 and 2.8 fold, respectively). Taken together, these data demonstrate that YFP receptor-chimera possess the same properties as their non-fluorescent counterparts.

### ***Monitoring 5-HT1A-mediated calcium signalling in living cells***

The 5-HT1A receptor has been shown to activate phospholipase C-mediated Ca<sup>2+</sup> release from the intracellular stores via G $\beta\gamma$ -subunits both in transfected as well as in cells endogenously expressing 5-HT1A (Aune et al., 1993; Liu and Albert, 1991; Pauwels and Colpaert, 2003). Therefore, functional coupling of WT-YFP and Mut-YFP receptors to calcium mobilization was examined by monitoring [Ca<sup>2+</sup>]<sub>i</sub> in transiently transfected in N1E-115 cells loaded with the fluorescent calcium chelator Fura-2AM. In addition to the receptors, cells were co-transfected with the functional G $\alpha_{i3}$ -CFP fusion protein (Leaney et al., 2002), which is resistant to the pertussis toxin (PTx), and treated with PTx to avoid the receptor-dependent activation of endogenous G<sub>i</sub>-proteins.

When the cells were transfected with recombinant  $G\alpha_{i3}$ -CFP protein in the absence of exogenous 5-HT1A receptor, no  $Ca^{2+}$  response was obtained after treatment of the cells with 8-OH-DPAT (Fig. 4A). Similar results were observed when  $G\alpha_{i3}$ -CFP was co-expressed with the 5-HT7-YFP receptor (data not shown). In contrast, co-expression of WT-YFP receptor with  $G\alpha_{i3}$ -CFP significantly increased fluorescence ratio  $F/F_0$  upon stimulation with 8-OH-DPAT, reflecting a rise in  $[Ca^{2+}]_i$  (Fig. 4B). Treatment of the co-transfected cells with the selective 5-HT1A receptor antagonist, WAY100635 at 1  $\mu$ M concentration blocked this effect, indicating that the increase in the  $Ca^{2+}$  concentration was specifically mediated by 5-HT1A receptor activation (Fig. 4C). Importantly, co-expression of the Mut-YFP receptor with  $G\alpha_{i3}$ -CFP did not produce any significant changes in the  $Ca^{2+}$  response after receptor stimulation with agonist (Fig. 4D).

#### ***5-HT1A-mediated redistribution of $G\alpha_i$ -proteins in living cells***

To study subcellular distribution of 5-HT1A-mediated signalling in real time, N1E-115 cells were transfected with the 5-HT1A-YFP receptors together with the functional  $G\alpha_{i3}$ -CFP fusion protein (Leaney et al., 2002). The  $G\alpha_{i3}$ -CFP protein also contains a C-terminal C-I mutation providing its resistance to the pertussis toxin (PTx). Coupling of the 5-HT1A receptor with endogenous  $G_{i/o}$ -proteins was disabled by treatment of transfected cells with PTx. Confocal microscopy of living cells revealed that both  $G\alpha_{i3}$ -CFP and 5-HT1A-YFP constructs were primarily distributed on the plasma membrane, where they were partly co-localised (Fig. 5A and 5B).

As shown in Figure 5A, treatment of cells expressing the WT-YFP receptor with 8-OH-DPAT results in a redistribution of the  $G\alpha_{i3}$ -CFP from the plasma membrane to the cytoplasm. Quantitative image analysis performed on the z-stack projections revealed approximately 2.5-fold increase in the fluorescence intensity ratio  $\Delta F/F_0$  for the  $G\alpha_{i3}$ -CFP

MOL #037085

within the cytoplasm in response to the agonist stimulation (Fig. 5C). In contrast, the fluorescence of the WT-YFP receptor was not significantly redistributed upon agonist stimulation (Fig. 5A). The receptor-dependent translocation of the  $G\alpha_{i3}$ -CFP was obtained in approximately 30% of transfected cells, indicating the importance of a proper stoichiometry between the signalling components. The agonist-dependent internalization of  $G\alpha_{i3}$ -CFP was specifically mediated by the 5-HT1A receptor, because it was blocked by the receptor specific antagonist WAY100635 (data not shown). Moreover, the agonist-dependent redistribution of the  $G\alpha_{i3}$ -CFP was not obtained in the absence of WT-YFP or in cells expressing YFP-tagged 5-HT7 receptor, which is known to activate stimulatory  $G_s$ -protein in response to 8-OH-DPAT (data not shown).

When acylation-deficient receptor mutant (Mut-YFP) was co-expressed together with  $G\alpha_{i3}$ -CFP in N1E-115 cells, their intracellular distribution was similar to that obtained for the cells co-transfected with WT-YFP receptor. However, there were no significant changes in localization of  $G\alpha_{i3}$ -CFP after stimulation of cells with 5-HT1A agonist 8-OH-DPAT (Fig. 5B and C).

To further examine the activation-dependent distribution of  $G\alpha_i$ , cellular fractionation of N1E-115 cells expressing either WT-YFP or Mut-YFP in addition to the  $G\alpha_{i3}$ -CFP was performed. The  $G\alpha_{i3}$ -CFP was visualized by immunoblotting of transfected and PTx treated cells with antibody directed against  $G\alpha_i$ -subunits, which allows parallel detection of endogenous  $G\alpha_i$ -proteins. Immunoblot analysis reveals that 8-OH-DPAT activation of the WT-YFP receptor causes a shift of  $G\alpha_{i3}$ -CFP from the particulate to the soluble fraction. In contrast, stimulation of the acylation-deficient, YFP-tagged receptor does not result in change of  $G\alpha_{i3}$ -CFP solubility (Fig. 5D). It is also notable that there was some translocation of the endogenous  $G\alpha_i$  proteins following receptor stimulation. These combined results demonstrate that stimulation of the 5-HT1A receptor leads to the translocation of  $G\alpha_i$ -subunits from the

membrane to the cytoplasm, and that receptor palmitoylation is critically involved in regulation of this event.

***Distribution of WT and palmitoylation-deficient 5-HT1A receptors within membrane subdomains (gradient centrifugation)***

Lipid modifications have been shown to play a role in the partitioning of several proteins into defined membrane subdomains, like lipid rafts and caveolae (Arni et al., 1998; Melkonian et al., 1999; Moffett et al., 2000). To determine, whether this may be the case for the 5-HT1A receptor, we compared the membrane distribution of the wild-type receptor and acylation-deficient mutant using density gradient centrifugation. To avoid artefacts resulting from overexpression, we generated NIH-3T3 cell lines stably expressing low amounts of WT-YFP ( $304 \pm 62$  fmol/mg) or Mut-YFP ( $605 \pm 64$  fmol/mg). These cells were solubilised in cold Triton X-100 and subjected to centrifugation in Optiprep™ density gradient in order to isolate detergent-insoluble membrane fractions. Immunoblot analysis of gradient fractions revealed that  $33 \pm 11\%$  ( $n = 4$ ) of the wild-type 5-HT1A receptor floated with the detergent-resistant low density fractions along with the caveolae-specific protein caveolin-1 and the  $\alpha_{i3}$ -subunit of heterotrimeric G-protein (Fig. 6A and C). When the NIH-3T3 cells stably expressing Mut-YFP were analysed, the yield of palmitoylation-deficient receptor in the light Triton X-100-resistant membrane fraction was reduced to  $4 \pm 3\%$  ( $n = 4$ ; Fig. 6B and C). It is also notable that distribution of the raft- as well as non-raft markers did not change in cell expressing Mut-YFP, when compared to the corresponding fractions generated from the WT-YFP expressing cells (Fig. 6D). Similar highly reproducible distribution patterns were also obtained in CHO cells transiently transfected with HA-tagged wild-type or acylation-deficient 5-HT1A receptors (not shown). This suggests that palmitoylation represents a targeting signal responsible for the partial localization of the 5-HT1A receptor in lipid rafts. This assumption was further supported by the observation that the pre-treatment of cells with methyl- $\beta$ -

cyclodextrin (M $\beta$ CD) significantly reduced the amount of WT-YFP receptor and G $\alpha_{i3}$ -subunit in the low density fractions (Fig. 7). The cholesterol-binding reagent M $\beta$ CD was previously shown to disrupt the cholesterol-enriched membrane subdomains by depletion of cholesterol from the plasma membrane (Harder et al., 1998).

***Distribution of WT and palmitoylation-deficient 5-HT1A receptors within membrane subdomains (co-patching of the 5-HT1A receptor with raft marker GM1)***

In addition to the gradient centrifugation experiments, we used fluorescence microscopy techniques to analyze the association of 5-HT1A receptor with lipid rafts on native plasma membrane sheets by using a copatching assay (Harder et al., 1998). Membrane sheets from the stably transfected NIH-3T3 cells were prepared by a brief ultrasound pulse, leaving behind the basal plasma membrane attached to the glass coverslip (Lang et al., 2001). After fixation of membrane sheets, lipid rafts were visualized by treatment with cholera toxin (CTX), which binds to the raft-associated ganglioside GM1. As shown in Figure 8A (*a to d*), both GM1 and 5-HT1A-YFP receptor signals were highly abundant and relative homogenous, thus not allowing to differentiate between specific and random colocalization. Therefore, segregation of the lipid rafts and receptors in more distinct domains was induced by incubating the native versus fixed membrane sheets with low concentrations of CTX and an anti-GFP antibody, respectively, in order to crosslink the corresponding domains (Spiegel et al., 1984). Such treatment resulted in the concentration of both labels in less numerous and clearly defined spots that were scattered over the membrane surface (Fig. 8A; *e to l*). It is also noteworthy that the depletion of cholesterol by treatment of the intact membrane sheets with M $\beta$ CD resulted in a more homogenous distribution of both receptor and GM1 fluorescence (Fig. 9). A similar distribution was also obtained in the absence of the crosslinking reagents (Fig. 9).

MOL #037085

A detailed analysis of the 5-HT<sub>1A</sub> receptor and GM1-derived fluorescence patterns revealed that 30.3±4.1% (n=3; in every repetition at least 10 different sheets were analyzed) of the wild-type receptor patches were also enriched with the lipid raft marker GM1. Importantly, this value was 3-fold reduced for the acylation-deficient mutant (Fig. 8B and C). These data demonstrate that a fraction of the 5-HT<sub>1A</sub> receptor is associated with the lipid rafts. These findings are also in line with the gradient centrifugation data suggesting the importance of palmitoylation for localization of the 5-HT<sub>1A</sub> receptor in the lipid rafts.

## DISCUSSION

The convenience of GFP labelling in combination with the recent advances in imaging techniques has not only allowed for qualitative, but also quantitative analysis of protein localization, trafficking and mobility in living cells (Chudakov et al., 2005). More specifically, fluorescence labelling of GPCRs represents a powerful tool for direct visualization of receptor-mediated signalling in real time (Kallal and Benovic, 2000; Milligan, 2004). In the present study we used YFP-tagged 5-HT<sub>1A</sub> receptor wild-type (WT-YFP) and its acylation-deficient mutant (Mut-YFP) to analyse their subcellular dynamics and to elucidate the role of receptor palmitoylation. Functionality of receptor-YFP constructs was assessed by the analysis of their subcellular distribution and by pharmacological studies. In addition, the efficiency of downstream signalling was tested by GTP $\gamma$ S binding assay as well as by receptor-dependent activation of extracellular signal-regulated kinases and Ca<sup>2+</sup> release. In all cases, YFP-chimera demonstrated similar responses as their non-fluorescent wild-type or acylation-deficient counterparts, indicating that YFP-fused receptors can be used in functional studies.

### *Dynamics of 5-HT<sub>1A</sub>-mediated signalling*

Since the components of the GPCR signalling cascade are expressed at relatively low concentration (Alousi et al., 1991; Milligan, 1996; Ostrom et al., 2000), their spatio-temporal organisation as well as activation-dependent dynamics are crucial determinants regulating the specificity and potency of signalling pathways. (Hur and Kim, 2002). In the present study we analysed the dynamic distribution of the serotonin-mediated signalling using YFP-fused 5-HT<sub>1A</sub> receptors and the functional G $\alpha_{i3}$ -CFP protein (Leaney et al., 2002). Time-lapse microscopy experiments demonstrated that in cells co-expressing WT-YFP and G $\alpha_{i3}$ -CFP, receptor stimulation resulted in translocation of the G $\alpha_{i3}$ -CFP from the plasma membrane to the cytoplasm. This observation was also consistent with cell fractionation experiments,

demonstrating an activation-induced shift of  $G\alpha_{i3}$ -CFP to the soluble fraction. These results extend previous data obtained with stimulatory  $G\alpha_s$ -protein, for which activation-mediated relocation from the particular to the soluble fraction has been demonstrated (Levis and Bourne, 1992; Wedegaertner et al., 1996). Such activation-dependent translocation of stimulatory  $G\alpha_s$ -subunit was recently directly confirmed by using functional  $G\alpha_s$ -GFP fusion protein (Yu and Rasenick, 2002). While true for  $G\alpha_s$  and, as shown in the present study, for  $G\alpha_{i/o}$  proteins, activation-mediated translocation of  $G\alpha$ -subunits seems to not be a general phenomenon. Experiments with  $G\alpha_q$  revealed that this G-protein is stably associated with the plasma membrane and agonist stimulation did not evoke its relocation (Hughes et al., 2001). One possible explanation for such discrepancies could be a different distribution of these G-proteins at the cell surface:  $G_i$ - and  $G_s$ -proteins have been shown to specifically concentrate in lipid raft domains, whereas  $G_q$  preferentially accumulates in caveolae via its specific interaction with caveolin (Oh and Schnitzer, 2001).

### ***Palmitoylation and localization of the 5-HT1A receptor in lipid microdomains***

We have previously demonstrated that the 5-HT1A receptor is palmitoylated at its C-terminal cysteine residues Cys417 and Cys420. Characterization of acylation-deficient 5-HT1A mutants revealed the importance of receptor palmitoylation for signaling (Papoucheva et al., 2004). However, molecular mechanisms by which palmitoylation may regulate receptor-dependent G-protein activation are still unknown. One possibility could be the involvement of 5-HT1A receptor palmitoylation in trafficking and/or localization of the receptor into specific membrane subdomains, like lipid rafts.

Protein modification by the covalent attachment of saturated fatty acyl chains, including myristic and palmitic acids represents one of the best characterised lipid raft targeting signals (Moffett et al., 2000; Zacharias et al., 2002). The long-chain fatty acids are

MOL #037085

expected to pack well in the  $l_o$  phase, increasing the avidity of protein for sphingolipid/cholesterol-enriched domains (Melkonian et al., 1999). Accordingly, a number of acylated proteins including heterotrimeric G-proteins  $\alpha$ -subunits, some Src family kinases, GAP-43 are resident in the lipid rafts (Arni et al., 1998; Melkonian et al., 1999; Moffett et al., 2000). It has been also shown that removal of the fatty acid modifications leads to the loss of the protein association with lipid rafts and caveolae (Moffett et al., 2000; Shaul et al., 1996; Shenoy-Scaria et al., 1994; Song et al., 1997). It is, however, noteworthy that the described results were mainly obtained with peripheral membrane proteins and cannot be simply extended to integral membrane proteins. The role of palmitoylation as a raft targeting signal for the latter remains controversial. For example, it has been shown that mutation of all palmitoylated cysteine residues on caveolin-1 does not affect its caveolae localization (Dietzen et al., 1995). On the other hand, reconstitution experiments have demonstrated that defined transmembrane peptides become excluded from  $l_o$  domains regardless of their acylation state (van Duyl et al., 2002). For the GPCRs, whose C-terminal intracellular domains are often palmitoylated, the role of acylation as a targeting signal for the rafts/caveolae localization has not been investigated so far. Several members of GPCR superfamily have been shown to be highly enriched in lipid rafts and caveolae, whereas others are present only in small amounts or excluded from the lipid rafts (Chini and Parenti, 2004).

In the present study we found that approximately 33% of the wild-type 5-HT<sub>1A</sub> receptor resides in the detergent-resistant membrane subdomains (DRMs). Cholesterol depletion results in solubilization of the 5-HT<sub>1A</sub> receptor, confirming association of the receptor with the cholesterol-enriched domains. DRM localization of the 5-HT<sub>1A</sub> was equally evident in different cell types (NIH-3T3 and CHO) suggesting that segregation of the receptor into lipid subdomains is intrinsic to the 5-HT<sub>1A</sub> itself. In contrast to the wild-type receptor, amount of acylation-deficient 5-HT<sub>1A</sub> receptor residing in TritonX-100 insoluble fractions

was significantly reduced, suggesting a functional involvement of receptor palmitoylation for the DRM trafficking.

Treatment of cells with non-ionic detergents at low temperature used in this study represents a classical approach for the DRM isolation. However, this method often produces controversial results and should not be expected to extract lipid rafts from cell membranes precisely (Simons and Vaz, 2004). Therefore, we used copatching as an additional assay to analyze the membrane distribution of the 5-HT<sub>1A</sub> receptor. This assay is based on the observation that two membrane components sharing a preference for lipid rafts will coalesce to form tightly associated patches after treatment with specific cross-linking reagents, like antibodies or multimeric toxins (Harder et al., 1998). Analysis of copatching data revealed that 30.3±4.1% of the 5-HT<sub>1A</sub> receptor was co-localized with the lipid raft ganglioside GM1. In contrast, the co-localization of the acylation-deficient mutant with the raft marker was drastically reduced. Thus, by using two independent methods we demonstrated that the significant fraction of the 5-HT<sub>1A</sub> receptor resides in lipid rafts in palmitoylation-dependent manner, demonstrate that stable palmitoylation of the 5-HT<sub>1A</sub> receptor represents an important targeting signal responsible for the localization of receptor in GM1-enriched membrane subdomains. Combined with our previous data on the signaling deficiency of non-palmitoylated 5-HT<sub>1A</sub> receptor, this finding also suggests that the palmitoylation-dependent raft localization of the receptor is involved in regulation of signaling processes.

How can palmitoylation-mediated localization of the 5-HT<sub>1A</sub> receptor in rafts be involved in regulation of the receptor activity? One possible scenario is that the irreversible receptor palmitoylation will accelerate the transient targeting of the receptor to lipid rafts. Such transient raft association may be further stabilized by the precoupling of the receptor with the G $\alpha_i$  protein (Emerit et al., 1990), which mainly resides in rafts (Oh and Schnitzer, 2001). Activation of the receptor will result in dissociation of the receptor bound G<sub>i</sub>-protein heterotrimeric complex thereby reducing the fraction of receptor interacting with G-protein

MOL #037085

(Janetopoulos et al., 2001). Such uncoupled receptors have been shown to possess increased mobility (Pucadyil et al., 2004) and could therefore leave the lipid microdomains by lateral diffusion. Outside of lipid rafts, the uncoupled 5-HT<sub>1A</sub> receptors become partly “non-functional” in terms of efficient signalling and need to undergo another cycle of raft localization to initialize activation of the G<sub>i</sub>-protein and downstream effectors upon stimulation. Several experimental observations support this model: *(i)* our data demonstrate that non-functional, acylation-deficient 5-HT<sub>1A</sub> mutant is excluded from DRMs, *(ii)* removal of cholesterol from hippocampal cells has been found to affect Gi-protein coupling of the 5-HT<sub>1A</sub> receptor and to affect the specific agonist binding (Pucadyil and Chattopadhyay, 2004) *(iii)* it has been shown that differently to other GPCRs, prolonged agonist stimulation of the 5-HT<sub>1A</sub> receptor does not result in considerable receptor internalization (Pucadyil et al., 2004; Riad et al., 2001).

## REFERENCES

- Alousi AA, Jasper JR, Insel PA and Motulsky HJ (1991) Stoichiometry of receptor-Gs-adenylate cyclase interactions. *Faseb J* **5**(9):2300-2303.
- Anderson RG (1998) The caveolae membrane system. *Annu Rev Biochem* **67**:199-225.
- Andrade R, Malenka RC and Nicoll RA (1986) A G protein couples serotonin and GABAB receptors to the same channels in hippocampus. *Science* **234**(4781):1261-1265.
- Arni S, Keilbaugh SA, Ostermeyer AG and Brown DA (1998) Association of GAP-43 with detergent-resistant membranes requires two palmitoylated cysteine residues. *J Biol Chem* **273**(43):28478-28485.
- Aune TM, McGrath KM, Sarr T, Bombara MP and Kelley KA (1993) Expression of 5HT1a receptors on activated human T cells. Regulation of cyclic AMP levels and T cell proliferation by 5-hydroxytryptamine. *J Immunol* **151**(3):1175-1183.
- Avery J, Ellis DJ, Lang T, Holroyd P, Riedel D, Henderson RM, Edwardson JM and Jahn R (2000) A cell-free system for regulated exocytosis in PC12 cells. *J Cell Biol* **148**(2):317-324.
- Brown DA and London E (1998) Functions of lipid rafts in biological membranes. *Annu Rev Cell Dev Biol* **14**:111-136.
- Burnet PW, Mefford IN, Smith CC, Gold PW and Sternberg EM (1996) Hippocampal 5-HT1A receptor binding site densities, 5-HT1A receptor messenger ribonucleic acid abundance and serotonin levels parallel the activity of the hypothalamo-pituitary-adrenal axis in rats. *Behav Brain Res* **73**(1-2):365-368.
- Chini B and Parenti M (2004) G-protein coupled receptors in lipid rafts and caveolae: how, when and why do they go there? *J Mol Endocrinol* **32**(2):325-338.
- Chudakov DM, Lukyanov S and Lukyanov KA (2005) Fluorescent proteins as a toolkit for in vivo imaging. *Trends Biotechnol* **23**(12):605-613.
- Claeysen S, Sebben M, Becamel C, Bockaert J and Dumuis A (1999) Novel brain-specific 5-HT4 receptor splice variants show marked constitutive activity: role of the C-terminal intracellular domain. *Mol Pharmacol* **55**(5):910-920.
- Cowen DS, Sowers RS and Manning DR (1996) Activation of a mitogen-activated protein kinase (ERK2) by the 5-hydroxytryptamine1A receptor is sensitive not only to inhibitors of phosphatidylinositol 3-kinase, but to an inhibitor of phosphatidylcholine hydrolysis. *J Biol Chem* **271**(37):22297-22300.
- De Vivo M and Maayani S (1986) Characterization of the 5-hydroxytryptamine 1a receptor-mediated inhibition of forskolin-stimulated adenylate cyclase activity in guinea pig and rat hippocampal membranes. *J Pharmacol Exp Ther* **238**(1):248-253.
- Dietzen DJ, Hastings WR and Lublin DM (1995) Caveolin is palmitoylated on multiple cysteine residues. Palmitoylation is not necessary for localization of caveolin to caveolae. *J Biol Chem* **270**(12):6838-6842.
- Dumuis A, Sebben M and Bockaert J (1988) Pharmacology of 5-hydroxytryptamine-1A receptors which inhibit cAMP production in hippocampal and cortical neurons in primary culture. *Mol Pharmacol* **33**(2):178-186.
- Emerit MB, el Mestikawy S, Gozlan H, Rouot B and Hamon M (1990) Physical evidence of the coupling of solubilized 5-HT1A binding sites with G regulatory proteins. *Biochem Pharmacol* **39**(1):7-18.
- Eroglu C, Brugger B, Wieland F and Sinning I (2003) Glutamate-binding affinity of Drosophila metabotropic glutamate receptor is modulated by association with lipid rafts. *Proc Natl Acad Sci U S A* **100**(18):10219-10224.
- Fargin A, Yamamoto K, Cotecchia S, Goldsmith PK, Spiegel AM, Lapetina EG, Caron MG and Lefkowitz RJ (1991) Dual coupling of the cloned 5-HT1A receptor to both

- adenylyl cyclase and phospholipase C is mediated via the same Gi protein. *Cell Signal* **3**(6):547-557.
- Foster LJ, De Hoog CL and Mann M (2003) Unbiased quantitative proteomics of lipid rafts reveals high specificity for signaling factors. *Proc Natl Acad Sci U S A* **100**(10):5813-5818.
- Garnovskaya MN, van Biesen T, Hawe B, Casanas Ramos S, Lefkowitz RJ and Raymond JR (1996) Ras-dependent activation of fibroblast mitogen-activated protein kinase by 5-HT<sub>1A</sub> receptor via a G protein beta gamma-subunit-initiated pathway. *Biochemistry* **35**(43):13716-13722.
- Gordon JA and Hen R (2004) The serotonergic system and anxiety. *Neuromolecular Med* **5**(1):27-40.
- Harder T, Scheiffele P, Verkade P and Simons K (1998) Lipid domain structure of the plasma membrane revealed by patching of membrane components. *J Cell Biol* **141**(4):929-942.
- Hughes TE, Zhang H, Logothetis DE and Berlot CH (2001) Visualization of a functional Galpha q-green fluorescent protein fusion in living cells. Association with the plasma membrane is disrupted by mutational activation and by elimination of palmitoylation sites, but not by activation mediated by receptors or AlF<sub>4</sub>. *J Biol Chem* **276**(6):4227-4235.
- Hur EM and Kim KT (2002) G protein-coupled receptor signalling and cross-talk: achieving rapidity and specificity. *Cell Signal* **14**(5):397-405.
- Janetopoulos C, Jin T and Devreotes P (2001) Receptor-mediated activation of heterotrimeric G-proteins in living cells. *Science* **291**(5512):2408-2411.
- Kallal L and Benovic JL (2000) Using green fluorescent proteins to study G-protein-coupled receptor localization and trafficking. *Trends Pharmacol Sci* **21**(5):175-180.
- Lang T, Bruns D, Wenzel D, Riedel D, Holroyd P, Thiele C and Jahn R (2001) SNAREs are concentrated in cholesterol-dependent clusters that define docking and fusion sites for exocytosis. *Embo J* **20**(9):2202-2213.
- Leaney JL, Benians A, Graves FM and Tinker A (2002) A novel strategy to engineer functional fluorescent inhibitory G-protein alpha subunits. *J Biol Chem* **277**(32):28803-28809.
- Levis MJ and Bourne HR (1992) Activation of the alpha subunit of G<sub>s</sub> in intact cells alters its abundance, rate of degradation, and membrane avidity. *J Cell Biol* **119**(5):1297-1307.
- Liu YF and Albert PR (1991) Cell-specific signaling of the 5-HT<sub>1A</sub> receptor. Modulation by protein kinases C and A. *J Biol Chem* **266**(35):23689-23697.
- Manes S, Ana Lacalle R, Gomez-Mouton C and Martinez AC (2003) From rafts to crafts: membrane asymmetry in moving cells. *Trends Immunol* **24**(6):320-326.
- Melkonian KA, Ostermeyer AG, Chen JZ, Roth MG and Brown DA (1999) Role of lipid modifications in targeting proteins to detergent-resistant membrane rafts. Many raft proteins are acylated, while few are prenylated. *J Biol Chem* **274**(6):3910-3917.
- Milligan G (1996) The stoichiometry of expression of protein components of the stimulatory adenylyl cyclase cascade and the regulation of information transfer. *Cell Signal* **8**(2):87-95.
- Milligan G (2004) Applications of bioluminescence- and fluorescence resonance energy transfer to drug discovery at G protein-coupled receptors. *Eur J Pharm Sci* **21**(4):397-405.
- Moffett S, Brown DA and Linder ME (2000) Lipid-dependent targeting of G proteins into rafts. *J Biol Chem* **275**(3):2191-2198.
- Nebigil CG, Garnovskaya MN, Casanas SJ, Mulheron JG, Parker EM, Gettys TW and Raymond JR (1995) Agonist-induced desensitization and phosphorylation of human 5-HT<sub>1A</sub> receptor expressed in Sf9 insect cells. *Biochemistry* **34**(37):11954-11962.

- Newman-Tancredi A, Verrielle L, Chaput C and Millan MJ (1998) Labelling of recombinant human and native rat serotonin 5-HT<sub>1A</sub> receptors by a novel, selective radioligand, [3H]-S 15535: definition of its binding profile using agonists, antagonists and inverse agonists. *Naunyn Schmiedebergs Arch Pharmacol* **357**(3):205-217.
- Oh P and Schnitzer JE (2001) Segregation of heterotrimeric G proteins in cell surface microdomains. G(q) binds caveolin to concentrate in caveolae, whereas G(i) and G(s) target lipid rafts by default. *Mol Biol Cell* **12**(3):685-698.
- Okamoto T, Schlegel A, Scherer PE and Lisanti MP (1998) Caveolins, a family of scaffolding proteins for organizing "preassembled signaling complexes" at the plasma membrane. *J Biol Chem* **273**(10):5419-5422.
- Ostrom RS, Post SR and Insel PA (2000) Stoichiometry and compartmentation in G protein-coupled receptor signaling: implications for therapeutic interventions involving G(s). *J Pharmacol Exp Ther* **294**(2):407-412.
- Overstreet DH (2002) Behavioral characteristics of rat lines selected for differential hypothermic responses to cholinergic or serotonergic agonists. *Behav Genet* **32**(5):335-348.
- Papoucheva E, Dumuis A, Sebben M, Richter DW and Ponimaskin EG (2004) The 5-hydroxytryptamine(1A) receptor is stably palmitoylated, and acylation is critical for communication of receptor with Gi protein. *J Biol Chem* **279**(5):3280-3291.
- Pauwels PJ and Colpaert FC (2003) Ca<sup>2+</sup> responses in Chinese hamster ovary-K1 cells demonstrate an atypical pattern of ligand-induced 5-HT<sub>1A</sub> receptor activation. *J Pharmacol Exp Ther* **307**(2):608-614.
- Pierce KL, Premont RT and Lefkowitz RJ (2002) SEVEN-TRANSMEMBRANE RECEPTORS. *Nat Rev Mol Cell Biol* **3**(9):639-650.
- Pucadyil TJ and Chattopadhyay A (2004) Cholesterol modulates ligand binding and G-protein coupling to serotonin(1A) receptors from bovine hippocampus. *Biochim Biophys Acta* **1663**(1-2):188-200.
- Pucadyil TJ, Kalipatnapu S, Harikumar KG, Rangaraj N, Karnik SS and Chattopadhyay A (2004) G-protein-dependent cell surface dynamics of the human serotonin 1A receptor tagged to yellow fluorescent protein. *Biochemistry* **43**(50):15852-15862.
- Radley JJ and Jacobs BL (2002) 5-HT<sub>1A</sub> receptor antagonist administration decreases cell proliferation in the dentate gyrus. *Brain Res* **955**(1-2):264-267.
- Riad M, Watkins KC, Doucet E, Hamon M and Descarries L (2001) Agonist-induced internalization of serotonin-1a receptors in the dorsal raphe nucleus (autoreceptors) but not hippocampus (heteroreceptors). *J Neurosci* **21**(21):8378-8386.
- Richter DW, Manzke T, Wilken B and Ponimaskin E (2003) Serotonin receptors: guardians of stable breathing. *Trends Mol Med* **9**(12):542-548.
- Sambrook J, Fritsch, E., Maniatis, T., ed. (1989) *Molecular cloning: a Laboratory Manual*. Cold Spring Harbour Laboratory press, Cold Spring Harbour, NY.
- Shaul PW, Smart EJ, Robinson LJ, German Z, Yuhanna IS, Ying Y, Anderson RG and Michel T (1996) Acylation targets endothelial nitric-oxide synthase to plasmalemmal caveolae. *J Biol Chem* **271**(11):6518-6522.
- Shenoy-Scaria AM, Dietzen DJ, Kwong J, Link DC and Lublin DM (1994) Cysteine<sup>3</sup> of Src family protein tyrosine kinase determines palmitoylation and localization in caveolae. *J Cell Biol* **126**(2):353-363.
- Sibille E and Hen R (2001) Serotonin(1A) receptors in mood disorders: a combined genetic and genomic approach. *Behav Pharmacol* **12**(6-7):429-438.
- Simons K and Toomre D (2000) Lipid rafts and signal transduction. *Nat Rev Mol Cell Biol* **1**(1):31-39.
- Simons K and Vaz WL (2004) Model systems, lipid rafts, and cell membranes. *Annu Rev Biophys Biomol Struct* **33**:269-295.

MOL #037085

- Song KS, Sargiacomo M, Galbiati F, Parenti M and Lisanti MP (1997) Targeting of a G alpha subunit (Gi1 alpha) and c-Src tyrosine kinase to caveolae membranes: clarifying the role of N-myristoylation. *Cell Mol Biol (Noisy-le-grand)* **43**(3):293-303.
- Spiegel S, Kassis S, Wilchek M and Fishman PH (1984) Direct visualization of redistribution and capping of fluorescent gangliosides on lymphocytes. *J Cell Biol* **99**(5):1575-1581.
- Sprong H, van der Sluijs P and van Meer G (2001) How proteins move lipids and lipids move proteins. *Nat Rev Mol Cell Biol* **2**(7):504-513.
- van Duyl BY, Rijkers DT, de Kruijff B and Killian JA (2002) Influence of hydrophobic mismatch and palmitoylation on the association of transmembrane alpha-helical peptides with detergent-resistant membranes. *FEBS Lett* **523**(1-3):79-84.
- Wedegaertner PB, Bourne HR and von Zastrow M (1996) Activation-induced subcellular redistribution of Gs alpha. *Mol Biol Cell* **7**(8):1225-1233.
- Yu JZ and Rasenick MM (2002) Real-time visualization of a fluorescent G(alpha)(s): dissociation of the activated G protein from plasma membrane. *Mol Pharmacol* **61**(2):352-359.
- Zacharias DA, Violin JD, Newton AC and Tsien RY (2002) Partitioning of lipid-modified monomeric GFPs into membrane microdomains of live cells. *Science* **296**(5569):913-916.

MOL #037085

## FOOTNOTES

U.R. and K.G. contributed equally to this paper. These studies were supported by the fund of the Medical School at the University of Göttingen and by the Deutsche Forschungsgemeinschaft through the Center of Molecular Physiology of the Brain to E.G.P. and Grant PO 732. We would like to thank Dr. Michael F.G. Schmidt for valuable discussions and suggestions regarding the manuscript.

## LEGENDS FOR FIGURES

### **Figure 1. Construction and expression of the YFP-tagged 5-HT1A receptors.**

(A) Schematic presentation of the wild-type and palmitoylation-deficient 5-HT1A receptors fused C-terminally with yellow fluorescent protein to produce WT-YFP and Mut-YFP constructs, respectively. C-terminal amino acid sequence of the 5-HT1A receptor is shown with a single-letter code. (B) Immunoblot analysis of YFP- and HA-tagged 5-HT1A receptors transiently expressed in N1E-115 cells. The blots were probed with antibodies directed against GFP or HA-tag. The molecular weight marker is indicated between the panels. (C) Cell surface proteins were labelled with sulfo-NHS-biotin and biotinylated proteins were isolated from the cell lysates with immobilized avidin. Biotinylated proteins were eluted and separated as described under *Materials and Methods*. Aliquots of unbound fractions and the eluates were analysed by SDS-PAGE and immunoblotting with anti-HA (*left*) or anti-GFP (*right*) antibodies. Representative immunoblots are shown. (D) Intracellular distribution of WT-YFP and Mut-YFP constructs. Representative confocal images obtained with LSM510-Meta microscope at 63x magnification are shown. Scale bar, 10  $\mu$ M.

### **Figure 2. Radioligand and [Eu]GTP $\gamma$ S binding studies of YFP-tagged 5-HT1A receptors.**

(A) Saturation binding analysis. The plots represent specific binding of agonist [ $^3$ H]8-OH-DPAT to WT-YFP, Mut-YFP and HA-WT. Radioligand binding assay was performed on membranes prepared from transfected NIH-3T3 cells. Data were fitted using the one-site saturation binding model and data points represent the means  $\pm$  S.E. from at least three independent experiments. (B) The [Eu]GTP $\gamma$ S binding response for HA-WT, WT-YFP and Mut-YFP was quantified at saturating concentration of 8-OH-DPAT (100  $\mu$ M) and [Eu]GTP $\gamma$ S binding for HA-WT receptor in the absence of ligand was set as 100 percent. Each value represents the mean  $\pm$  S.E. from three independent experiments. (C) Dose-response curves for ligand-induced G $\alpha_{i3}$ -protein activation. [Eu]GTP $\gamma$ S binding to plasma

MOL #037085

membranes was measured with varying concentrations of 8-OH-DPAT after immunoprecipitation with anti-G $\alpha_{i3}$  antibody. In several experiments WAY100635 (1 $\mu$ M) was added to the membranes 5 min before agonist. Background fluorescence from non-transfected cells was subtracted before the analysis. Data points represent the means  $\pm$  S.E. from three independent experiments. F.U., fluorescence units.

**Figure 3. Activation of Erk by YFP-tagged 5-HT1A receptors** (A) NIH-3T3 cells expressing YFP- or HA-tagged 5-HT1A receptors were treated for 5 minutes with 10  $\mu$ M 8-OH-DPAT or vehicle, separated by SDS/PAGE and then subjected to immunoblot either with antibodies raised either against total (*upper panel*) or phosphorylated (*lower panel*) Erk. Fluorograms are representative of three independent experiments. (B) Quantification of Erk phosphorylation was performed by densitometry and calculated as the ratio of total Erk expression over the Erk phosphorylation signal. Each value represents the mean  $\pm$  S.E. (n = 3). A statistically significant difference between values is noted (\*, p < 0.05)

**Figure 4. 5-HT1A receptor-mediated changes in intracellular Ca<sup>2+</sup> concentration.** Neuroblastoma N1E-115 cells were transiently transfected with YFP-tagged 5-HT1A receptors and G $\alpha_{i3}$ -CFP construct. Changes in [Ca<sup>2+</sup>]<sub>i</sub> were measured using calcium indicator FURA-2AM. Cells co-expressing YFP-tagged receptor and G $\alpha_{i3}$ -CFP were selected by fluorescence microscopy with appropriate excitation and emission filter sets. Activity of endogenous G<sub>i</sub>-proteins was blocked by the overnight pre-treatment of cells with PTx (100 ng/ml). Data are representative of four independent experiments and every trace corresponds to one measured cell. (A) Ca<sup>2+</sup> response in N1E-115 cells transfected with G $\alpha_{i3}$ -CFP construct alone. (B) Cells co-expressing WT-YFP and G $\alpha_{i3}$ -CFP showed increase in intracellular Ca<sup>2+</sup> concentration after stimulation of receptor with 8-OH-DPAT. (C) Pre-

MOL #037085

treatment of cells co-transfected with  $G\alpha_{i3}$ -CFP and WT-YFP constructs with 5-HT1A antagonist WAY100635 blocked 8-OH-DPAT-induced  $Ca^{2+}$  response. **(D)** In cells expressing acylation-deficient Mut-YFP receptor together with the  $G\alpha_{i3}$ -CFP no increase in  $[Ca^{2+}]_i$  was induced upon receptor stimulation.

**Figure 5. Translocation of  $G\alpha_{i3}$ -CFP fusion protein in the living N1E-115 cells upon activation of the 5-HT1A receptor.** Cells were co-transfected with  $G\alpha_{i3}$ -CFP protein and either with WT-YFP or Mut-YFP receptors and viewed by confocal microscopy. To block coupling of receptor to endogenous  $G_i$ -proteins, cells were treated with pertussis toxin. Images were assembled at 10-s intervals and the specific 5-HT1A receptor agonist 8-OH-DPAT was added at the time point 0. Representative confocal images obtained with LSM510-Meta at magnification of 63x are shown for cells expressing WT-YFP receptor together with  $G\alpha_{i3}$ -CFP **(A)** or acylation-deficient Mut-YFP construct together with  $G\alpha_{i3}$ -CFP **(B)**. Scale bar, 10  $\mu$ m **(C)** Quantitative image analysis of cells before and during treatment with 8-OH-DPAT. Changes in CFP-fluorescence intensity within the cytoplasm were calculated as described under *Materials and Methods*. A statistically significant difference between values is noted (\*\*,  $p < 0.01$ ). Each value represents the mean  $\pm$  S.E. from at least three independent experiments **(D)** Cellular fractionation of N1E-115 cells expressing either WT-YFP or Mut-YFP together with  $G\alpha_{i3}$ -CFP. Activity of endogenous  $G_i$ -proteins was blocked by pre-treatment of cells with PTx. Transfection cells were treated with 8-OH-DPAT for 30 s, rapidly harvested and the content of  $G\alpha_{i3}$ -CFP (*upper panel*) as well as endogenous  $G\alpha_{i3}$  (*lower panel*) in soluble and membrane fractions was examined by immunoblot analysis.

**Figure 6. Localization of the wild-type and acylation-deficient 5-HT1A receptors in the detergent-resistant membrane fractions (DRMs).** The NIH-3T3 cells stably expressing

MOL #037085

either the WT-YFP (**A**) or the Mut-YFP (**B**) were lysed with the cold 1% Tryton-X100 and lysates were ultracentrifugated in the Optiprep™ density gradient. The gradient fractions were analysed by immunoblotting. G $\alpha_i$  protein and caveolin-1 were used as DRM markers while transferrin receptor (TfR) was used as the non-DRM marker. (**C**) Relative amount of the receptor in the high density fractions (35%+40%) and the buoyant low density fractions (25%+30%). Quantitative analysis of the receptor distribution was performed by densitometry and calculated in percentage of the total protein amount in all fractions. Data points represent mean  $\pm$  S.E. (n = 4). A statistically significant difference between values is noted (\*, p < 0.05) (**D**) Relative amount of the caveolin-1, G $\alpha_i$  and transferrin receptor (TfR) in the high density fractions (35%+40%) and the buoyant low density fractions (25%+30%). Data points represent mean  $\pm$  S.E. (n = 3).

**Figure 7. Cholesterol depletion reduces localization of the WT-YFP and the G $\alpha_i$  in the DRMs.** The NIH-3T3 cells ( $1 \times 10^6$ ) stably expressing the WT-YFP were treated with 10 mM M $\beta$ CD for 45 minutes or left untreated (*w/o* M $\beta$ CD), lysed with cold 1% Tryton-X100 and subjected to the ultracentrifugation in the Optiprep™ density gradient. The gradient fractions were analysed by SDS-PAGE and immunoblotting. Representative fluorogram is shown (n=3).

**Figure 8. Copatching of WT-YFP and Mut-YFP receptors with lipid raft ganglioside GM1.** (**A**) Copatching assay was performed in plasma membrane sheets derived from the stably transfected NIH-3T3 cells. (a,e and i) Staining of the membrane lipids with TMA-DPH (*blue*). (b,f and j) Copatching of 5-HT1A-YFP receptors with anti-GFP antibody (*green*). (c,g and l) Copatching of GM1 with cholera toxin. GM1 patches were detected using Alexa546 anti-CTX antibody (*red*). (d,h and l) The merge of receptor and GM1 signals. (a-d) Membrane sheets were fixed before incubation with anti-GFP antibody and CTX. (e-l) Membrane sheets were fixed after incubation with anti-GFP antibody and CTX. Circles mark the fluorescent

MOL #037085

beads which were used to align images obtained in different fluorescence channels for quantitative analysis. **(B)** Example of the line scans analysis for regions 1 and 2, which are shown with arrows in (I). Fluorescence intensity was analysed pixel by pixel along the line applied on the merge pictures. When the distance between the maximal values obtained for green and red fluorescence was less than two pixels, a co-localization event was counted (*upper panel*). Otherwise, patches were counted as non colocalized (*lower panel*). **(C)** Quantitative analysis of co-localization events between WT-YFP or Mut-YFP and GM1. Data points represent mean  $\pm$  S.E. (n = 3). A statistically significant difference between values is noted (\*\*,  $p < 0.01$ ).

**Figure 9.** (a-d) Distribution of WT-YFP and ganglioside GM1 in the membrane sheets in the absence of the crosslinking reagents. Copatching assay was performed on fixed plasma membrane sheets derived from the stably transfected NIH-3T3 cells after 60 minutes of incubation in KGlu buffer at 37°C without antibodies and without the cholera toxin. (e-h) Distribution of WT-YFP and ganglioside GM1 after cholesterol depletion with methyl- $\beta$ -dextran. Methyl- $\beta$ -dextran was applied in concentration of 5 mM for 10 minutes and copatching was performed as described under *Materials and Methods*. (a and e) Staining of the membrane lipids with TMA-DPH. (b and f) Copatching of 5-HT<sub>1A</sub>-YFP receptors with anti-GFP antibody. (c and g) Copatching of GM1 with cholera toxin. GM1 patches were detected using Alexa546-labeled anti-CTX antibody. (d and h) The merge of receptor and GM1 signals.

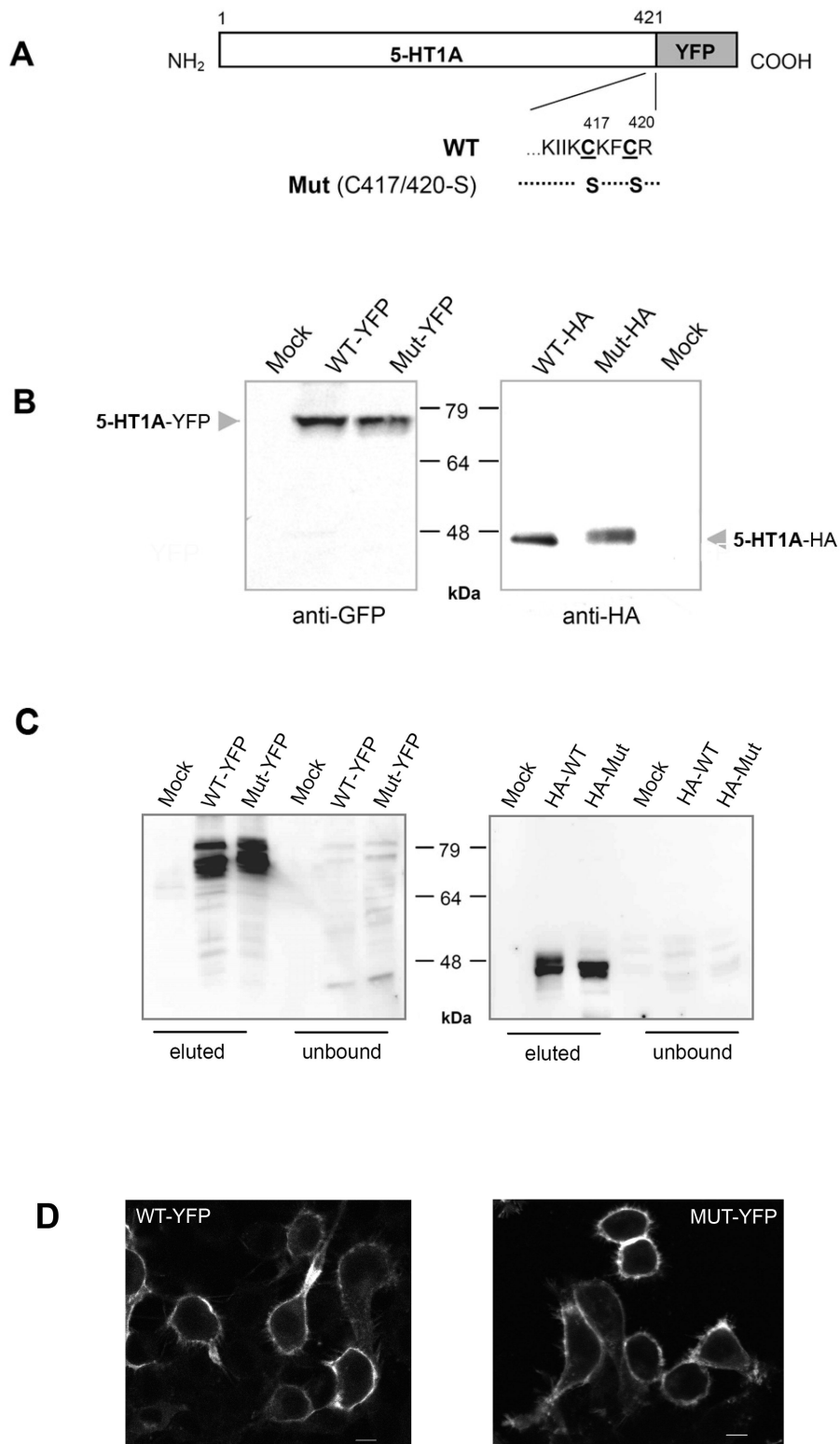


Figure 1

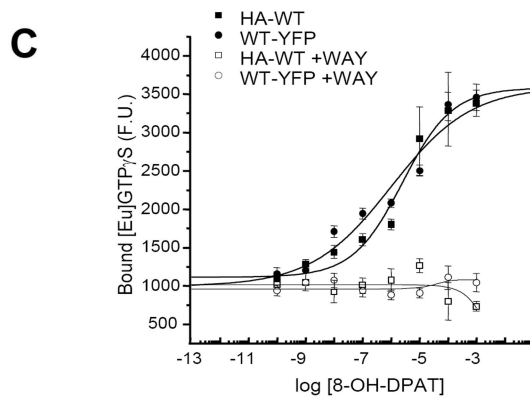
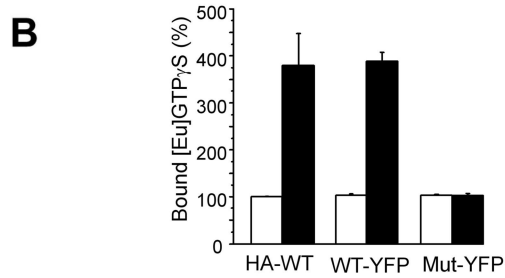
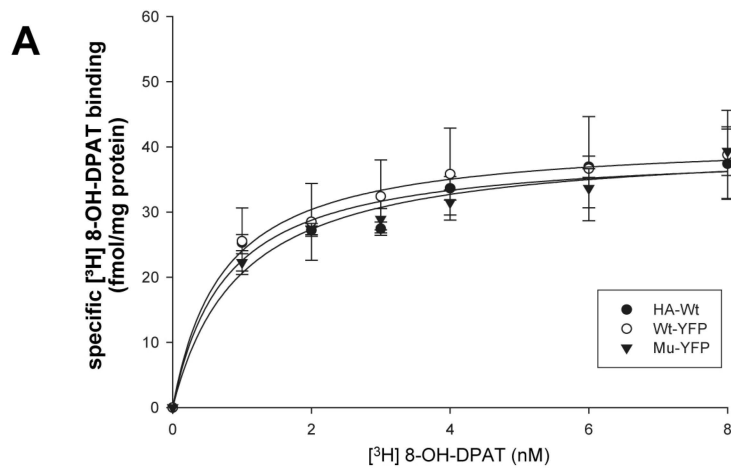
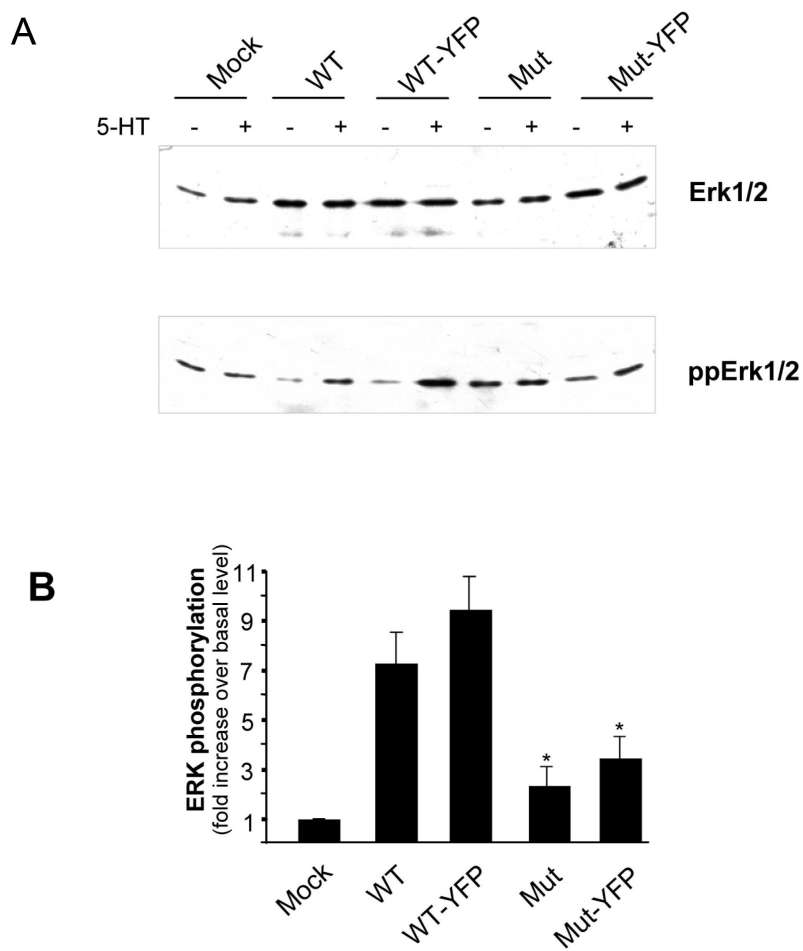


Figure 2



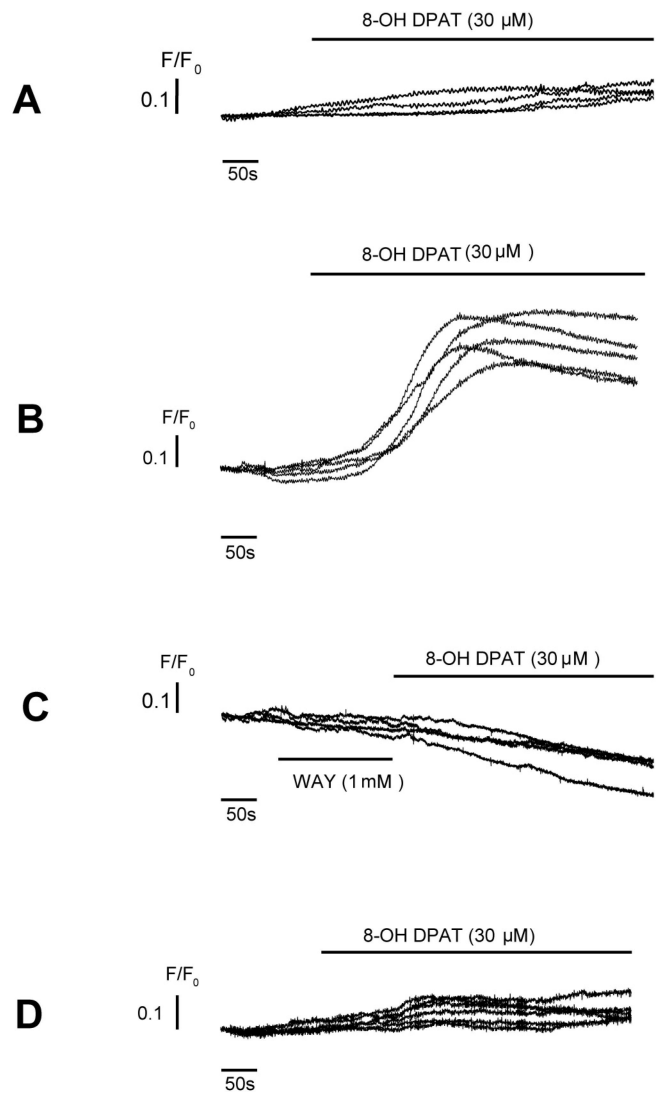


Figure 4

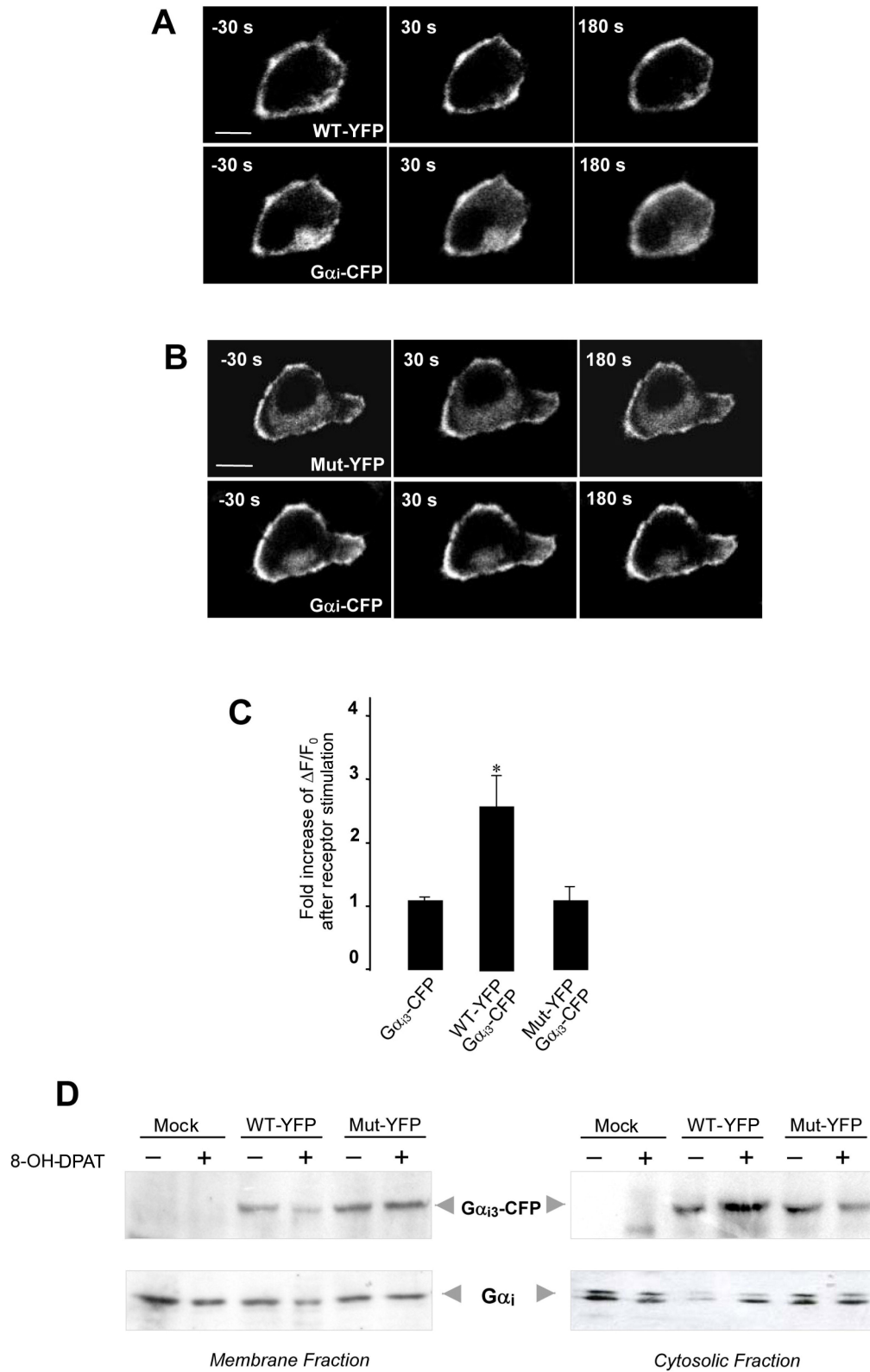


Figure 5

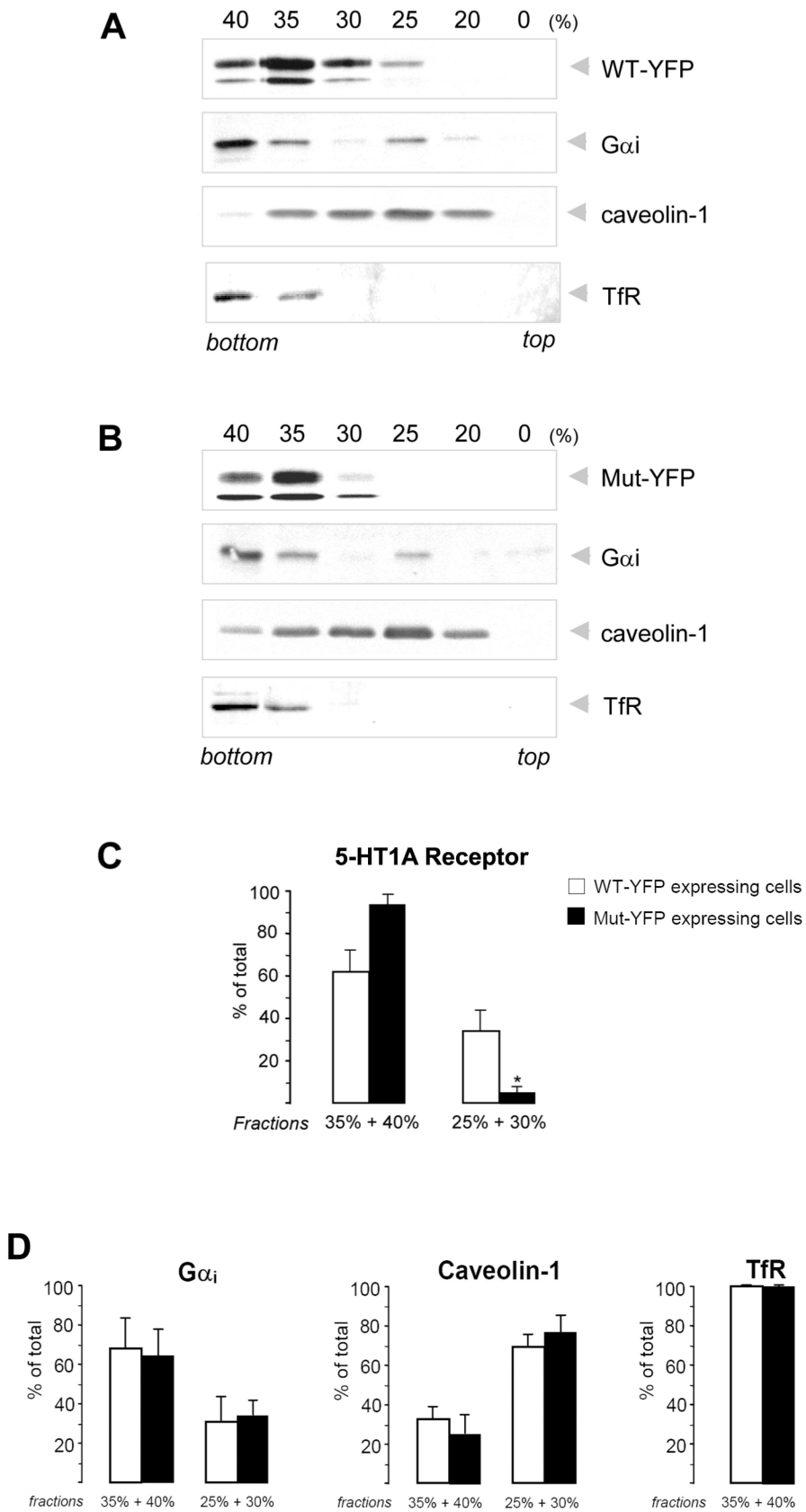


Figure 6

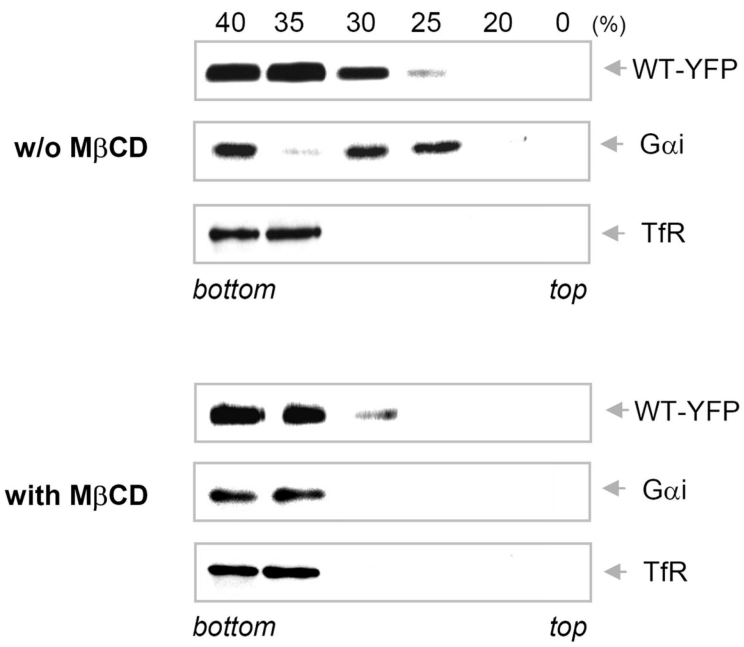


Figure 7

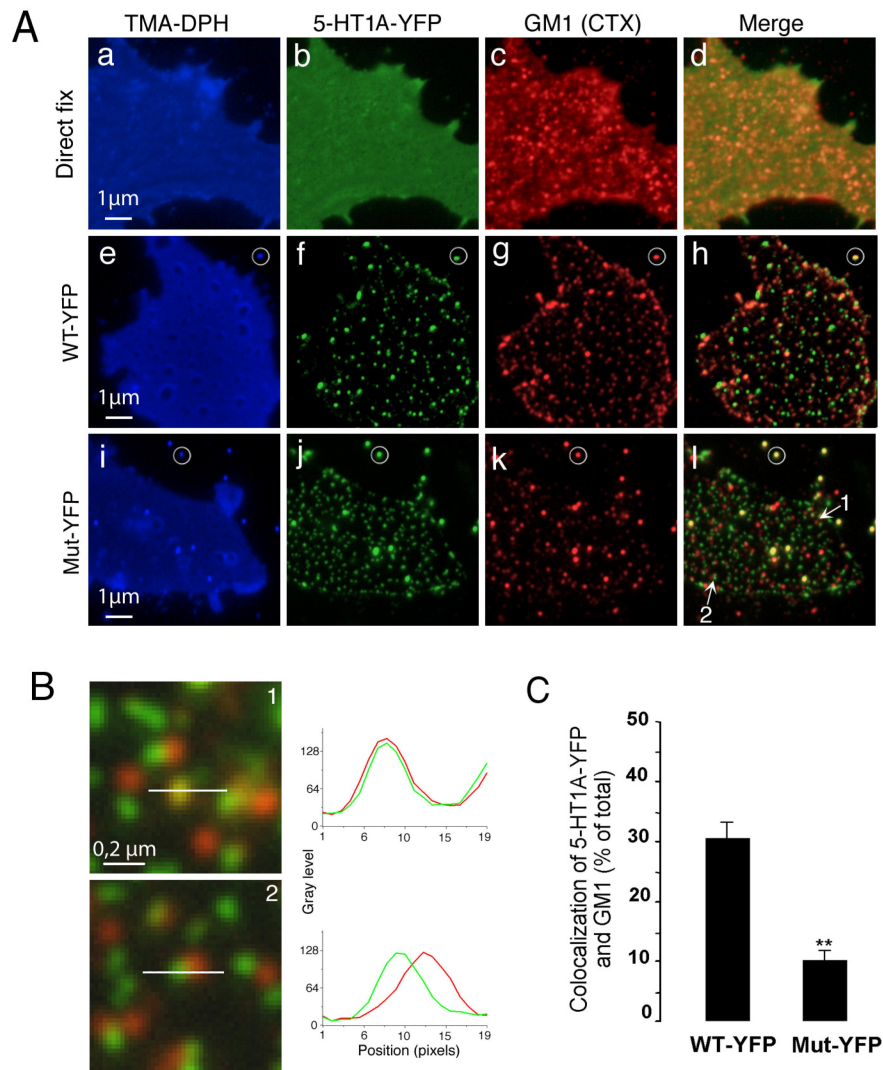


Figure 8

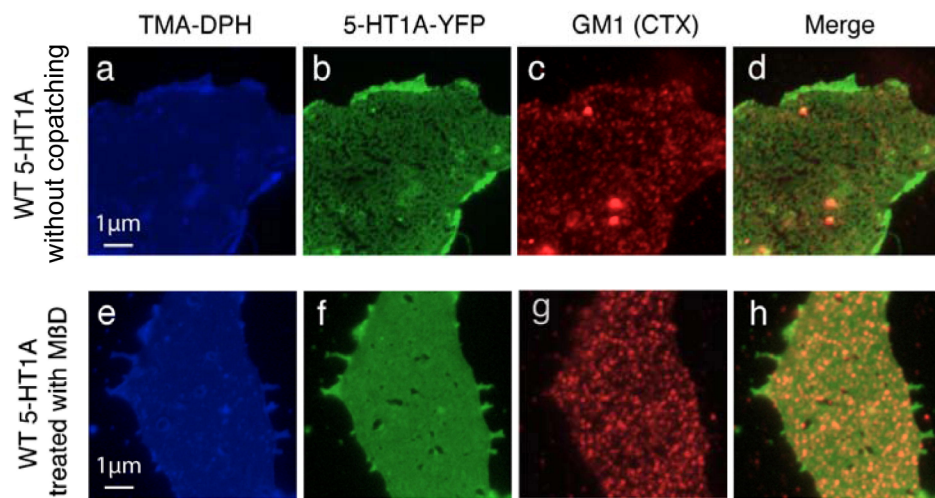


Figure 9